JOURNAL OF APPLIED POLYMER SCIENCE VOL. 19, 2473–2484 (1975)

Reverse Osmosis Separations of Aldehydes, Ketones, and Ethers in Aqueous Solutions Using Porous Cellulose Acetate Membranes

TAKESHI MATSUURA, M. E. BEDNAS, J. M. DICKSON,* and S. SOURIRAJAN, *Division of Chemistry, National Research Council of Canada, Ottawa, Canada*

Synopsis

Reverse osmosis data for a number of aldehyde, ketone, and ether solutes whose polar parameters $\Sigma\sigma^*$ lie in the ranges of −0.2 to 0.6, −0.4 to 0.6, and −0.49 to 0.6, respectively, have been analyzed. The results show that solute transport parameters can be expressed as a function of steric parameter ΣE_s only for ethers, polar parameter $\Sigma\sigma^*$ only for aldehydes, and both ΣE_s and $\Sigma\sigma^*$ for ketones. The numerical values of the functional proportionality constants ρ^* and δ^* associated with $\Sigma\sigma^*$ and ΣE_s, respectively, for the above class of solutes have been determined for operating pressures up to 500 psig, and a method of predicting solute separation from data on any reference solute only in each class has been established. The data on solute transport parameters for ethers, aldehydes, and ketones have been correlated with the corresponding data for sodium chloride through appropriate link constants. Analysis of data on mixed solute systems involving aldehydes and ketones show that the solutes behave independently in reverse osmosis.

INTRODUCTION

The physical chemistry of the Taft and Hammett equations representing the effect of structure on the reactivity of molecules is extensively dscussed in the literature.[1–7] The relevance of the polar (Hammett's number $\Sigma\sigma$, and Taft's number $\Sigma\sigma^*$) and steric (Taft's number ΣE_s) parameters to reverse osmosis separation of organic solutes in aqueous solutions using porous cellulose acetate membranes has been established in a series of papers.[8–12] It may be recalled that unique correlations exist between the values of $\Sigma\sigma^*$ and those of $\Delta\nu_s$ (acidity) and $\Delta\nu_s$ (basicity) for different organic molecules representing their hydrogen bonding abilities, and pK_a values of different organic solutes representing their dissociation equilibrium constants.[8–10] The values of $\Sigma\sigma^*$ and ΣE_s have also been correlated uniquely with data on equilibrium and rate constants involving a wide variety of reactions.[1] It has been reported[2] that 42000 equilibrium and rate constants are encompassed by the Hammett equation. Also, Charton has demonstrated that Taft's E_s constants are a linear function of the van der Waals radii, and hence they are a true measure of steric effects. Such correlations give both a thermodynamic and mechanistic basis for the above polar and steric parameters. Further, the Taft and Hammett equations have been used to correlate uniquely a large number of funda-

*Co-op student, Department of Chemical Engineering, University of Waterloo, Canada

mental physicochemical quantities including dipole moments, bond energies, ionization potentials, polarographic half-wave potentials, infrared absorption frequencies, wavelength of ultraviolet spectra, and some nuclear magnetic resonance and nuclear quadrupole coupling data. On the basis of the foregoing characteristics of the polar ($\Sigma\sigma$ and $\Sigma\sigma^*$) and the steric (ΣE_s) parameters, it is reasonable to conclude that the above parameters, and the correlations governed by these parameters, have a uniquely fundamental physicochemical significance in terms of the effect of structure on the reactivity of organic molecules.

The effects of Taft's polar parameter $\Sigma\sigma^*$ and steric parameter ΣE_s on reverse osmosis separations of alcohols, aldehydes, ketones, and noncyclic ethers in aqueous solutions involving single solute systems and porous cellulose acetate membranes have been discussed.[11,12] On the basis of the above effects, methods of predicting reverse osmosis separations of single and mixed alcohols in aqueous solutions have been established and illustrated.[11] Extending the above work, this paper illustrates the predictability of the reverse osmosis separations of aldehydes, ketones, and noncyclic ethers in single and mixed solute systems. The solute transport parameters for the above class of solutes are also correlated with those for sodium chloride in the manner illustrated earlier[11] for alcohol solutes.

EXPERIMENTAL

Reverse osmosis separations of seven ethers, six aldehydes, and seven ketones, listed in Table I, were studied in this work. The apparatus used and

TABLE I
Physicochemical Data of Solutes[a]

No.	Solute: Name	Solute: Formula	Mol. wt	σ^* or $\Sigma\sigma^*$	E_s or ΣE_s
	Ethers	R_1, R_2 in R_1—O—R_2			
1	*t*-Butyl isopropyl ether	*t*-C_4H_9, i-C_3H_7	116.2	−0.490	−2.24
2	*t*-Butyl ethyl ether	*t*-C_4H_9, C_2H_5	102.2	−0.400	−1.61
3	Diisopropyl ether	i-C_3H_7, i-C_3H_7	102.2	−0.380	−1.40
4	Butyl ethyl ether	*n*-C_4H_9, C_2H_5	102.2	−0.230	−0.46
5	Dipropyl ether	*n*-C_3H_7, *n*-C_3H_7	102.2	−0.230	−0.72
6	Phenetole	C_2H_5, C_6H_5	122.2	+0.500	−0.13
7	Anisole	CH_3, C_6H_5	108.1	+0.600	−0.06
	Aldehydes	R in RCHO			
1	Isobutyraldehyde	i-C_3H_7	72.1	−0.190	−0.70
2	Isovaleraldehyde	i-C_4H_9	86.1	−0.200	−0.93
3	*n*-Butyraldehyde	*n*-C_3H_7	72.1	−0.115	−0.36
4	Propionaldehyde	C_2H_5	58.1	−0.100	−0.07
5	Acetaldehyde	CH_3	44.1	0	0
6	Benzaldehyde	C_6H_5	106.1	+0.60	−0.06
	Ketones	R_1, R_2 in R_1—C(=O)—R_2			
1	Diisopropyl ketone	i-C_3H_7, i-C_3H_7	114.2	−0.380	−1.40
2	Diisobutyl ketone	i-C_4H_9, i-C_4H_9	142.2	−0.400	−1.86
3	Cyclopentanone	cyclo-C_4H_8	84.1	−0.250	−0.51
4	Methyl isopropyl ketone	CH_3, i-C_3H_7	86.1	−0.190	−0.70
5	Methyl isobutyl ketone	CH_3, i-C_4H_9	100.2	−0.200	−0.93
6	Methyl ethyl ketone	CH_3, C_2H_5	72.1	−0.100	−0.07
7	Acetone	CH_3, CH_3	58.1	0	0

[a] Data for $\Sigma\sigma^*$ and ΣE_S are taken from refs. 1 and 12.

TABLE II
Film Specifications

Film no.	1	2	3	5	6	7	8	9	11	12
	250 psig[a]					500 psig[a]				
Pure water permeability constant A, $\frac{\text{g-mole } H_2O}{\text{cm}^2 \text{ sec atm}} \times 10^6$	1.61	2.09	2.61	3.62	7.27	1.58	2.04	2.58	3.25	5.87
Solute transport parameter $(D_{AM}/K\delta)_{NaCl}$, cm/sec $\times 10^5$	2.10	3.82	5.52	19.82	152.9	2.98	5.02	6.25	20.97	124.3
Solute separation, %	95.0	93.5	90.7	77.6	47.8	96.0	93.9	92.9	79.3	48.5
Product rate, g/hr[b]	21.4	27.4	34.2	47.6	98.6	43.7	55.8	67.5	88.7	162.4

[a] Operating pressure.

[b] Area of film surface = 13.2 cm²; feed solution 1500 ppm NaCl–H_2O; mass transfer coefficient $k = 22 \times 10^{-4}$ cm/sec.

the experimental details were the same as those reported earlier.[11,12] Batch 316 (10/30)-type cellulose acetate membranes[13] were used at the operating pressures of 250 and 500 psig. The specifications of the membranes used are given in Table II in terms of pure water permeability constant A (in g mole H_2O/cm² sec atm) and solute transport parameter $(D_{AM}/K\delta)$ (in cm/sec) for sodium chloride at the above operating pressures. Table II also includes some data on membrane performance at the operating pressures of 250 and 500 psig using 1500 ppm NaCl–H_2O feed solutions. The feed concentrations for the organic solutes used were in the range of 0.0006 to 0.0098 g-mole/l.; in most cases, the solute concentration in the feed was ~200 ppm. In all cases, the osmotic pressure of the feed solution was negligible compared to the operating pressure, and the rate of membrane-permeated solution (product rate) was nearly the same as the pure-water permeation rate. All experiments were of the short-run type, and they were carried out at the laboratory temperature (23–25°C). The concentrations of organic solutes were determined by gas-chromatographic analysis details of which have been reported earlier.[12] The fraction solute separation f in each experiment was obtained from the relation

$$f = \frac{\text{solute ppm in feed} - \text{solute ppm in product}}{\text{solute ppm in feed}} \quad (1)$$

Except for some of the data at 500 psig, which were taken from the earlier paper,[12] all the other data used in this paper were obtained from experiments at 250 and 500 psig carried out specifically for the purpose of this work. All the data at 500 psig taken from the earlier paper were reanalyzed with the new data at 250 psig and additional data at 500 psig. This accounts for the slight differences in the values of ρ^* and δ^* reported in this paper.

RESULTS AND DISCUSSION

Analysis of Data

Using the experimental solute separation f and product rate (PR) (in g/hr per given area of membrane surface) data, the solute transport parameter $(D_{AM}/K\delta)$ (in cm/sec) for each solute was calculated as before[12] from the relation

$$(D_{AM}/K\delta) = \frac{(PR)}{3600\ S\ d}\frac{(1-f)}{f}\left[\exp\left\{\frac{(PR)}{3600\ S\ k\ d}\right\}\right]^{-1} \quad (2)$$

where S = effective membrane area (cm^2), d = solution density (g/cm^3), and k = mass transfer coefficient (in cm/sec) on the high-pressure side of the membrane. The numerical values of k under the experimental conditions used were taken as the same as those given in reference 12. The $(D_{AM}/K\delta)$ data so obtained were then subjected to least-squares or multiple regression analysis for linear correlation in terms of one of the following equations, as indicated for each class of solutes on the basis of the earlier work[12]:

$$(D_{AM}/K\delta)_{\text{ether}} = C^* \quad \exp(\delta^*\Sigma E_s) \quad (3)$$

$$(D_{AM}/K\delta)_{\text{aldehyde}} = C^* \quad \exp(\rho^*\Sigma\sigma^*) \quad (4)$$

$$(D_{AM}/K\delta)_{\text{ketone}} = C^* \quad \exp(\rho^*\Sigma\sigma^* + \delta^*\Sigma E_s) \quad (5)$$

where $\Sigma\sigma^*$ and ΣE_s are the Taft polar and steric parameters for the substituent group in the solute molecule; ρ^* and δ^* are the functional proportionality constants associated with $\Sigma\sigma^*$ and ΣE_s, respectively; and C^* is an overall proportionality constant relating $(D_{AM}/K\delta)$ and $\exp(\rho^*\ \Sigma\sigma^*)$ and/or $\exp(\delta^*\Sigma E_s)$. It is important to note that the numerical value of C^* is not the same in all the three eqs. (3), (4), and (5); the numerical value of C^* is a function of the porous structure and chemical nature of the membrane surface as well as the chemical nature of the functional group in the solute molecule, in addition to the other experimental conditions.

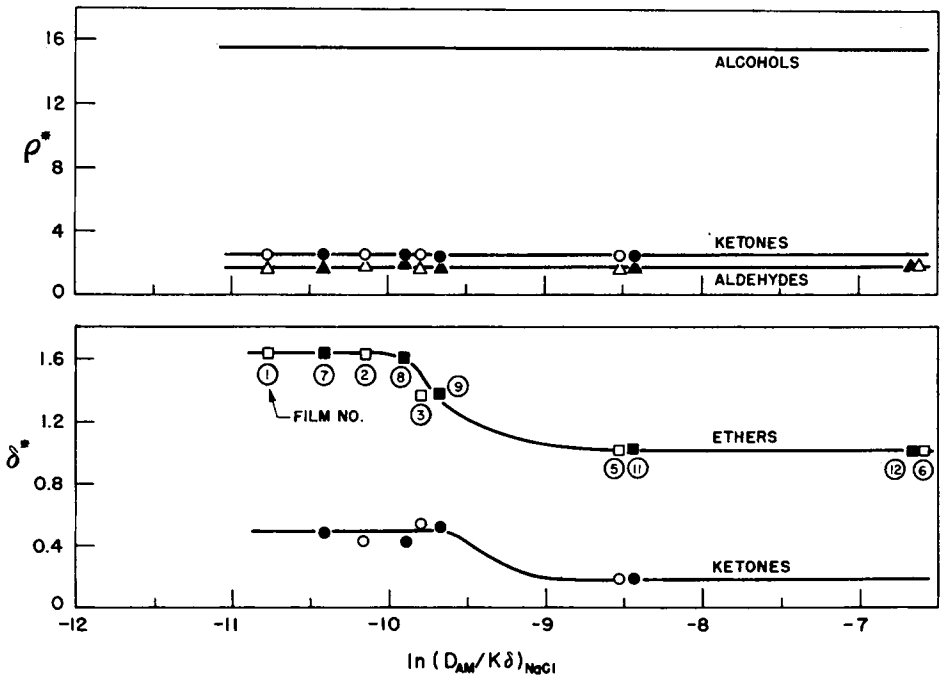

Fig. 1. Effect of pore size on membrane surface on ρ^* and δ^* for alcohols, ethers, aldehydes, and ketones. Film type, cellulose acetate, Batch 316(10/30); operating pressure, 250 psig (open symbol) and 500 psig (closed symbol): (□, ■) ethers; (△, ▲) aldehydes; (○, ●) ketones.

TABLE III
Reverse Osmosis Characteristics of Cellulose Acetate Membranes at Operating Pressures of 500 psig or Less

Characteristic of solute molecule				δ *	
				ln ($D_{AM}/K\delta$) for NaCl for the membrane[a]	
Polar functional group	$\Sigma\sigma$* range	ΣE_s range	ρ*	>−8.5	<−10.0
Alcohols	−0.3 to 0	−1.54 to 0	15.5	0	0
Aldehydes	−0.2 to 0.6	−0.93 to 0	1.7	0	0
Ketones	−0.4 to 0.6	−1.86 to 0	2.5	0.19	0.49
Ethers (noncyclic)	−0.49 to 0.6	−2.24 to −0.06	0	1.02	1.64

[a] When ln ($D_{AM}/K\delta$) for NaCl for the membrane is in the range <−8.5 and >−10.0, the value of δ * increases steeply with decrease in pore size.

From the above correlations, the values of ρ* and δ* were obtained for each class of solutes as a function of operating pressure and average pore size on the membrane surface as expressed by ($D_{AM}/K\delta$) data for sodium chloride at the operating pressure.

The results of the above analysis are given in Figure 1. The results show that the values of ρ* and δ* (which are different for different classes of solutes) are essentially the same at both the operating pressures studied. While the values of ρ* are independent of the pore size on the membrane surface, those of δ* are dependent on such pore size. The data given in Figure 1 may be considered to represent the reverse osmosis characteristics of cellulose acetate membranes of the type used in this work for the separations of alcohols, aldehydes, ketones, and ethers in aqueous solutions. For practical purposes, these characteristics may be stated in terms of the applicable values of ρ* and δ* given in Table III.

Predictability of Solute Separations

The data on ρ* and δ* given in Table III can be used to predict reverse osmosis separations for the indicated classes of solutes from experimental data obtained for a single reference solute in each class for any given membrane. This was tested in this work with particular reference to the separations of ethers, aldehydes, and ketones listed in Table I, using the following form of eq. (2):

$$f = \left[1 + (D_{AM}/K\delta)\frac{\exp(v_s/k)}{v_s}\right]^{-1} \tag{6}$$

where

$$v_s = \frac{(PR)}{3600\ S\ d}. \tag{7}$$

For the purpose of this test, t-butyl ethyl ether, isobutyraldehyde, and diisopropyl ketone were arbitrarily chosen as the reference solutes for ethers, aldehydes, and ketones, respectively. The values of k given in reference 12

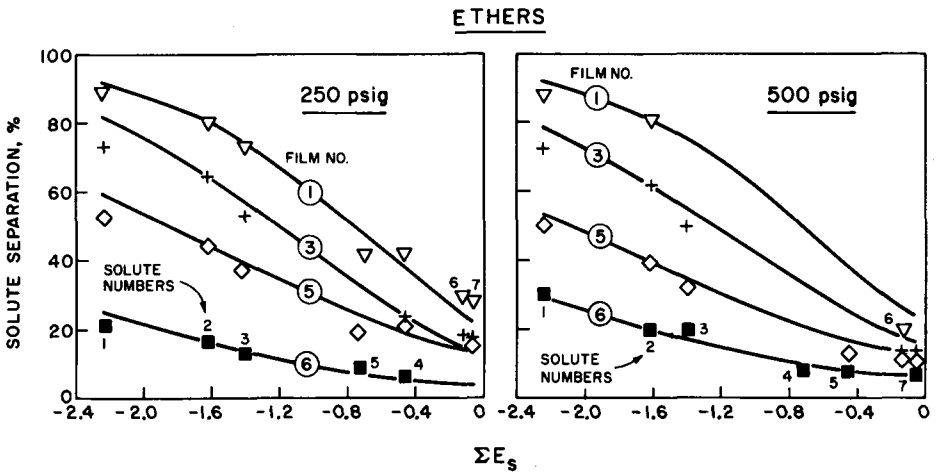

Fig. 2. Effect of ΣE_s on solute separation of ethers for films 1, 3, 5, and 6: (——) predicted; (▽ + ◇, ■) experimental. Film type, cellulose acetate, Batch 316(10/30); operating pressure, 250 and 500 psig; feed concentration, 0.0013 ~0.0075 g-mole/l.; flow rate, 400 cc/min; membrane area, 13.2 cm^2; solute numbers, same as in Table I.

were used in the prediction calculations for the experimental conditions used in this work. The calculation procedure used in predicting solute separations was as follows.

From the experimental solute separation *(f)* and product rate *(PR)* data, calculate $(D_{AM}/K\delta)$ and the quantity v_s using eqs. (2) and (7), respectively, for each of the reference solution system. The numerical value of $(D_{AM}/K\delta)$ is different for different solutes; the value of the quantity v_s may be considered to be essentially constant in view of the very dilute feed solutions involved.

Using the above values of $(D_{AM}/K\delta)$ for each of the reference solutes, and their values of $\Sigma\sigma^*$ and/or ΣE_s given in Table I, and the applicable values of

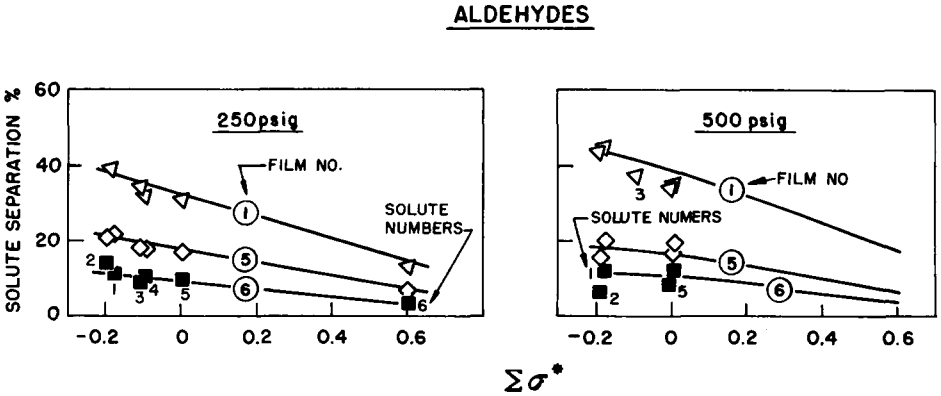

Fig. 3. Effect of $\Sigma\sigma^*$ on solute separation of aldehydes for films 1, 5, and 6: (——) predicted; (▽, ◇, ■) experimental. Film type, cellulose acetate, Batch 316(10/30); operating pressure, 250 and 500 psig; feed concentration, 0.0019 ~0.0098 g-mole/l.; flow rate, 400 cc/min; membrane area, 13.2 cm^2; solute numbers, same as in Table I.

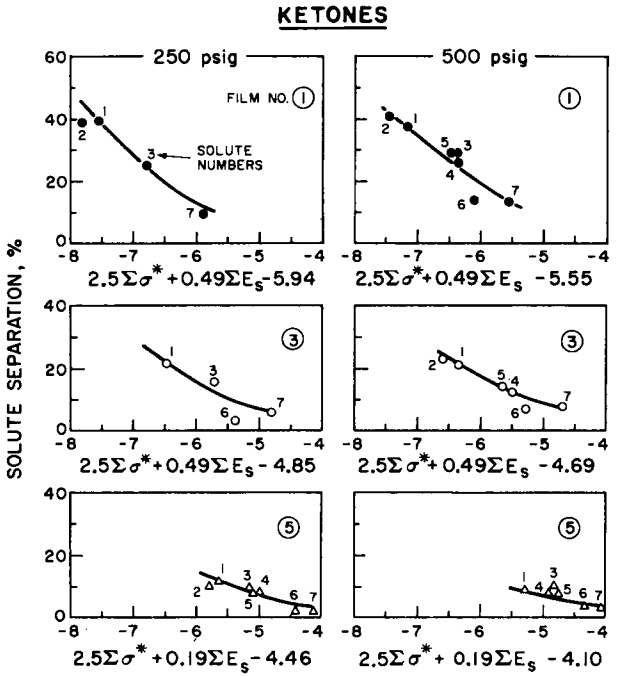

Fig. 4. Effect of ($\rho^*\Sigma\sigma^* + \delta^*\Sigma E_s + \ln C^*$) on solute separation of ketones for films 1, 3, and 5: (——) predicted; (●, ○, △) experimental. Film type, cellulose acetate, Batch 316(10/30); operating pressure, 250 and 500 psig; feed concentration, 0.0006 ~0.0035 g-mole/l.; flow rate, 400 cc/min; membrane area, 13.2 cm^2; solute numbers, same as in Table I.

ρ^* and δ^* given in Table III and Figure 1, calculate C^* corresponding to each reference system using the appropriate equation from the set of eqs. (3) to (5). Each value of C^* so calculated may be assumed constant for all systems involving solutes with the functional group same as that of the reference solute.

Using the above values of C^* and the appropriate equation from the set of eqs. (3) to (5) and the data given in Tables I and III and Figure 1, calculate the values of $(D_{AM}/K\delta)$ for all the other solutes in Table I.

Using the above values of $(D_{AM}/K\delta)$, calculate solute separations for all the other solutes using eq. (6).

TABLE IV
Comparison of Calculated and Experimental Reverse Osmosis Separations of Ethers at 375 psig[a]

Solute no.	Solutes	ΣE_S	Film no.	Solute separation, %	
				Experimental	Calculated
2	*t*-Butyl ethyl ether	−1.61	7	90.4	88.2
4	Butyl ethyl ether	−0.46	7	45.5	48.0
			9	21.1	19.3
7	Anisole	−0.06	9	14.3	13.0

[a] Reference: dipropyl ether (solute no. 5); film: CA Batch 316(10/30); solute concentration: 0.002 g-mole/l.

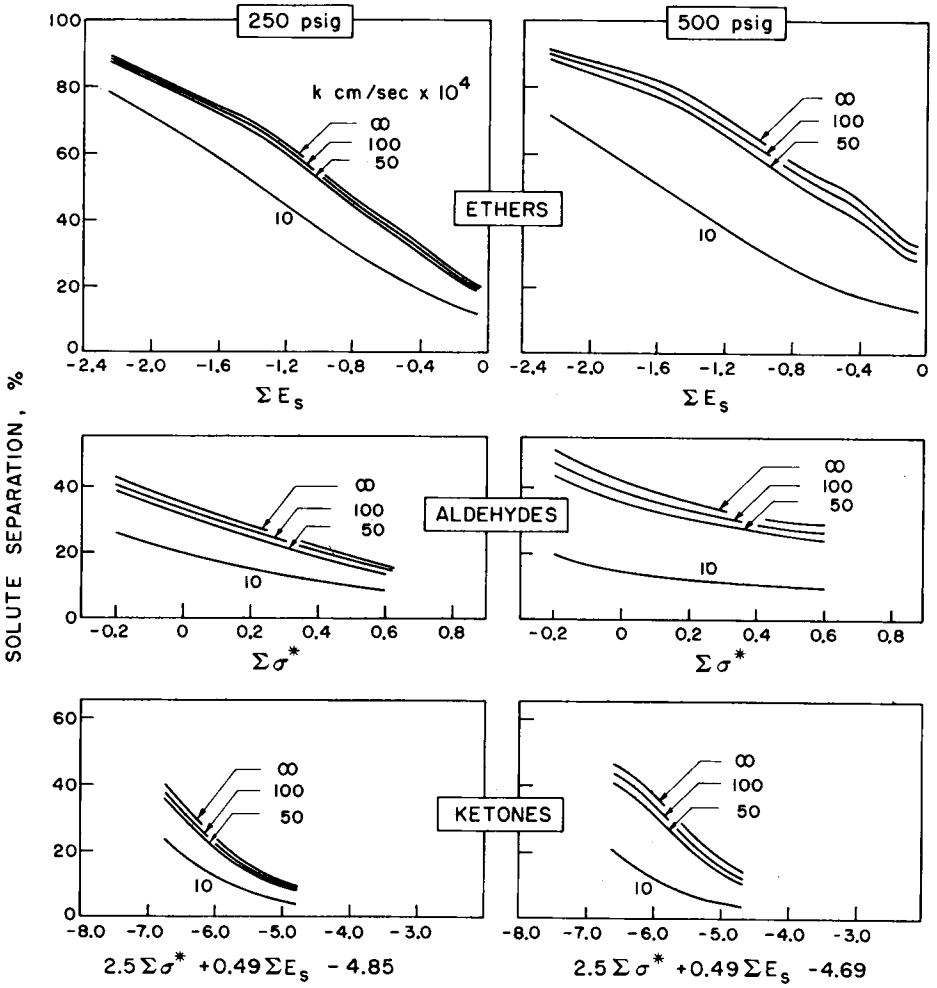

Fig. 5. Effect of mass transfer coefficient k on solute separations for ethers, aldehydes, and ketones. Film type, cellulose acetate, Batch 316(10/30); operating pressure, 250 and 500 psig; film 3 specified in Table II.

The data on solute separation calculated by the above procedure (solid lines) are given in Figures 2, 3, and 4 along with corresponding experimental data (points) at the operating pressures of 250 and 500 psig. Table IV gives some additional calculated and experimental results carried out at 375 psig. All data show excellent agreement between calculated and experimental results confirming the validity of ρ^* and δ^* values given in Table III.

Equation (6) also offers a means of predicting the effect of mass transfer coefficient k on solute separation f. This is illustrated in Figure 5 with respect to film 3, which shows the variations in solute separations of ethers, aldehydes, and ketones for $k \times 10^4$ (in cm/sec) values of 10, 50, 100, and ∞. Solute separations decrease with decrease in k; the decrease in solute separation is relatively more at higher operating pressures, and at values of k less than 50×10^{-4} cm/sec at each operating pressure. These results are similar to those reported earlier for the separations of alcohols.[11]

Figure 5 shows that for practical purposes, it is desirable to obtain a k value of 50×10^{-4} cm/sec or more, for good use of available membranes from the point of view of obtaining high solute separations. Many alcohols, aldehydes, and ketones are known to exist in fruit juices as flavor components.[14] In the concentration of fruit juices by reverse osmosis, the value of k usually obtained is $\sim 10 \times 10^{-4}$ cm/sec or less.[14,15] From the effect of k on solute separations given in Figure 5, it is clear that such low mass transfer coefficient is a major reason for low separations of flavor components during reverse osmosis concentration of fruit juices.

It has been shown already that when $(D_{AM}/K\delta)$ and k remain constant, solute separation will pass through a maximum when $(v_s/k) = 1$. For the condition $k = 10 \times 10^{-4}$ cm/sec, the values of (v_s/k) for film 3 at 250 and 500 psig were 0.804 and 1.44, respectively. Assuming that $(D_{AM}/K\delta)$ values are essentially constant in the above pressure range, one can expect that solute separation to pass through a maximum at a pressure intermediate between 250 and 500 psig for the condition $k = 10 \times 10^{-4}$ cm/sec.

Correlations of Relative Solute Transport Parameters for Ethers, Aldehydes, and Ketones with Those for Sodium Chloride

Figure 6 gives a plot of the relative values of the solute transport parameter for NaCl, $(D_{AM}/K\delta)_{NaCl}$, versus ln C^* for ethers, aldehydes, and ketones obtained with five films of different surface porosities. The figure includes data for both operating pressures 250 and 500 psig. The straight-line correlation given for alcohols represents the data reported in the earlier work.[11] In Figure 6, the data for $(D_{AM}/K\delta)_{NaCl}$ used were those directly obtained from experiments. The ln C^* values were determined from experimental reverse osmosis data for the reference solutes mentioned earlier.

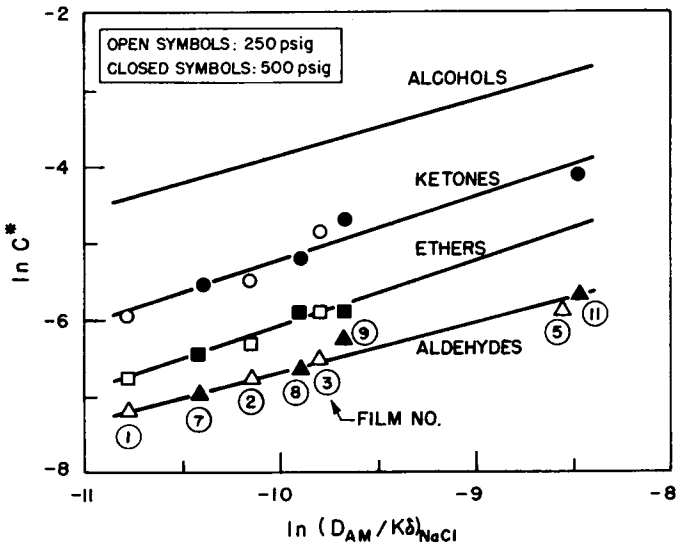

Fig. 6. Correlation of ln C^* for alcohols, ethers, aldehydes, and ketones vs. ln $(D_{AM}/K\delta)$ for sodium chloride. Film type, cellulose acetate, Batch 316(10/30); operating pressure, 250 psig (open symbol) and 500 psig (closed symbol); (□, ■) ethers; (△, ▲) aldehydes; (○, ●)ketones.

Figure 6 shows that for the membranes whose ln $(D_{AM}/K\delta)_{NaCl}$ values are in the range of −8.2 to −10.8, the ln $(D_{AM}/K\delta)_{NaCl}$ versus ln C^* correlation is essentially a straight line for ethers, aldehydes, and ketones; and in each case, the correlating straight line is identical for both the operating pressures used.

It may be recalled[11] that ln C^* = ln $(D_{AM}/K\delta)_{solute}$ when $\Sigma E_s = 0$ and $\Sigma\sigma^*$ and 0, with reference to ether, aldehyde, and ketone solutes. The linear correlations given in Figure 6 can be used as before[11] to link the values of $(D_{AM}/K\delta)$ for the ether, aldehyde, and ketone solutes with those of $(D_{AM}/K\delta)_{NaCl}$. Equations (3), (4), and (5) can be rewritten as follows:

$$\ln\ (D_{AM}/K\delta)_{ether} = \delta^*\Sigma E_s + \ln\ C^* \tag{8}$$

$$\ln\ (D_{AM}/K\delta)_{aldehyde} = \rho^*\Sigma\sigma^* + \ln\ C^* \tag{9}$$

$$\ln\ (D_{AM}/K\delta)_{ketone} = \rho^*\Sigma\sigma^* + \delta^*\Sigma E_s + \ln\ C^* \tag{10}$$

On the basis of Figure 6, let

$$\ln\ C^* = a_{ether}\ \ln\ (D_{AM}/K\delta)_{NaCl} + \ln\ b_{ether} \tag{11}$$

$$\ln\ C^* = a_{aldehyde}\ \ln\ (D_{AM}/K\delta)_{NaCl} + \ln\ b_{aldehyde} \tag{12}$$

and

$$\ln\ C^* = a_{ketone}\ \ln\ (D_{AM}/K\delta)_{NaCl} + \ln\ b_{ketone}. \tag{13}$$

Equations (11), (12), and (13) are applicable to ether, aldehyde, and ketone solutes, and the quantities a and ln b are the corresponding link constants.

Equations (8), (9), and (10) can then be written as

$$\ln\ (D_{AM}/K\delta)_{ether} = a_{ether}\ \ln\ (D_{AM}/K\delta)_{NaCl} + \delta^*\Sigma E_s + \ln\ b_{ether} \tag{14}$$

$$\ln\ (D_{AM}/K\delta)_{aldehyde} = a_{aldehyde}\ \ln\ (D_{AM}/K\delta)_{NaCl} + \rho^*\Sigma\sigma^* + \ln\ b_{aldehyde} \tag{15}$$

and

$$\ln\ (D_{AM}/K\delta)_{ketone} = a_{ketone}\ \ln\ (D_{AM}/K\delta)_{NaCl} + \rho^*\Sigma\sigma^* + \delta^*\Sigma E_s + \ln\ b_{ketone}. \tag{16}$$

Equations (14), (15), and (16) link the values of $(D_{AM}/K\delta)$ for ethers, aldehydes, and ketones with those of $(D_{AM}/K\delta)_{NaCl}$ through the link constants a and ln b and the parameters δ^* and ΣE_s, and ρ^* and $\Sigma\sigma^*$. The values of a and ln b were evaluated by the least-squares treatment of data on $(D_{AM}/K\delta)_{NaCl}$ and ln C^* values for ethers, aldehydes, and ketones, respectively. The results were

$$a_{ether} = 0.453,\ \ln\ b_{ether} = -1.65$$

$$a_{aldehyde} = 0.645,\ \ln\ b_{aldehyde} = -0.21$$

$$a_{ketone} = 0.818,\ \ln\ b_{ketone} = 2.96.$$

The values of a and ln b given above for ethers, aldehydes, and ketones together with data on ρ^*, $\Sigma\sigma^*$, δ^*, and ΣE_s offer a means of predicting ln $(D_{AM}/K\delta)$ for any solute listed in Table I from data on $(D_{AM}/K\delta)_{NaCl}$ alone for any

membrane whose surface porosity is in the range covered in Figure 6, at any operating pressure up to 500 psig.

Effect of Mixed Solutes on Solute Separation

The effect of mixed solutes on membrane performance was ascertained by reverse osmosis experiments using several membrane samples of different surface porosities. The following mixed-solute systems were studied: diisopropyl ketone + diisobutyl ketone; methyl ethyl ketone + acetone; and isobutyraldehyde + diisopropyl ketone. The solute concentration used was 0.00067 to 0.0052 g-mole/l. with respect to each solute. The operating pressure used was 250 psig in all cases. The product rate obtained in each experiment for a given membrane was essentially the same. With respect to solute separation, the data obtained for the separations of diisopropyl ketone, diisobutyl ketone, methyl ethyl ketone, acetone, and isobutyraldehyde in mixed-solute systems were compared with the corresponding data obtained in single-solute systems. The results, some of which are given in Table V, showed that within the limits of experimental error, the separations for each solute in single- and mixed-solute systems were essentially identical, indicating that the above solutes behave independently in reverse osmosis. A similar conclusion was reached earlier[11] with respect to alcohol solutes. These results are of practical significance in fruit juice concentration by reverse osmosis.

CONCLUSIONS

The effects of Taft's polar parameter $\Sigma\sigma^*$ and steric parameter ΣE_s on reverse osmosis separations of alcohols, aldehydes, ketones, and ethers have been illustrated. On the basis of the above effects, methods of predicting reverse osmosis separations of the above classes of compounds have been illustrated for both single and mixed solute systems. For purposes of predicting membrane performance, the applicable values of the polar and steric functional constants ρ^* and δ^* have also been determined for each class of the above solutes for operating pressures up to 500 psig. These results make a

TABLE V
Comparison of Solute Separation in Single-Solute System with Corresponding Data in Mixed-Solute System[a]

Film No.	Mixed-solute systems	Solute separation, %		Solute separation, %, for single-solute system	
	Solute systems[b] A & B	A	B	A	B
2	Diisopropyl ketone	34.8	29.6	32.0	29.4
3	and diisobutyl ketone	22.4	16.3	21.5	16.5
1	Methyl ethyl ketone	9.7	8.9	7.7	8.9
5	and acetone	0.5	0.4	1.2	2.2
2	Isobutyraldehyde and	34.9	34.4	33.6	32.0
	diisobutyl ketone	9.2	4.0	11.1	4.2

[a] Film type: CA Batch 316(10/30).
[b] System type: A-B-H_2O; solute concentration: 0.00067 ~ 0.0052 g-mole/l.

significant contribution to the engineering science of reverse osmosis transport with respect to porous cellulose acetate membranes.

Issued as N.R.C. No. 14759.

References

1. R. W. Taft, Jr., in *Steric Effects in Organic Chemistry,* M. S. Newman, Ed., Wiley, New York, 1956, pp. 556–675.
2. H. H. Jaffe, *Chem. Rev.*, **53,** 191 (1953).
3. P. R. Wells, *Chem. Rev.*, **63,** 171 (1963).
4. C. K. Ingold, *Structure and Mechanism in Organic Chemistry,* 2nd ed., Cornell University Press, Ithaca, N.Y., 1969, p. 1192.
5. M. Charton, *J. Amer. Chem. Soc.*, **91,** 615 (1969).
6. J. Shorter, in *Advances in Linear Free Energy Relationships,* N. B. Chapman and J. Shorter, Eds., Plenum Press, London and New York, 1972, pp. 72–117.
7. M. Charton, *Chemtech,* August 502 (1974).
8. T. Matsuura and S. Sourirajan, *J. Appl. Polym. Sci.*, **15,** 2905 (1971).
9. T. Matsuura and S. Sourirajan, *J. Appl. Polym. Sci.*, **16,** 1663 (1972).
10. T. Matsuura and S. Sourirajan, *J. Appl. Polym. Sci.*, **17,** 1043 (1973).
11. T. Matsuura, M. E. Bednas, and S. Sourirajan, *J. Appl. Polym. Sci.*, **18,** 567 (1974).
12. T. Matsuura, M. E. Bednas, J. M. Dickson, and S. Sourirajan, *J. Appl. Polym. Sci.*, **18,** 2829 (1974).
13. L. Pageau and S. Sourirajan, *J. Appl. Polym. Sci.*, **16,** 3185 (1972).
14. T. Matsuura, A. G. Baxter, and S. Sourirajan, *Acta Alimentaria,* **2,** 109 (1973).
15. T. Matsuura, A. G. Baxter, and S. Sourirajan, *J. Food Sci.*, **39,** 704 (1974).

Received December 13, 1974
Revised January 27, 1975